Bath-induced delocalization in interacting disordered spin chains

Dries Sels

Phys. Rev. B **106**, L020202 — Published 27 July 2022

DOI: 10.1103/PhysRevB.106.L020202

Bath induced delocalization in interacting disordered spin chains

Dries Sels[1, 2]

[1] *Department of Physics, New York University, New York, NY, USA*
[2] *Center for Computational Quantum Physics, Flatiron Institute, New York, NY, USA*

(Dated: July 20, 2022)

Over a decade of work has culminated in the consensus that one-dimensional systems, subject to sufficiently large disorder fail to thermalize and posses an extensive set of local integrals of motion. In this work I will provide numerical evidence for the contrary. In particular, this paper studies the dynamics of disordered spin chains which are weakly coupled to a Markovian bath. Within this approach, the critical disorder for stability to quantum avalanches exceeds $W^* \gtrsim 20$ in the random field Heisenberg chain. In stark contrast to the Anderson insulator, the avalanche threshold drifts considerably with system size, with no evidence of saturation in the studied regime.

To date, the putative many-body localized (MBL) phase is the sole example of a generic interacting local Hamiltonian system that fails to thermalize under its own internal dynamics. In contrast to other non-ergodic systems, the integrability of the MBL phase is *emergent*, induced simply by strong disorder in the local potential energy. As such, the phenomenon has attracted a lot attention from the community over the past decade [1, 2]. After the initial proposal [3–5], research has been primarily focused on understanding the nature of the phase transition between the thermal and the MBL phase. A rather complete picture seemed to have emerged, supporting an MBL phase in one dimension. Recently, the debate about the stability of the MBL phase has been revived due to inconsistencies between the prevailing theory and new numerical experiments [6–16]. Most of these numerical experiments were done at relative weak disorder in, or in the vicinity of, the thermal phase. This has raised some criticism and the question whether this bias somehow affects the conclusion. In this context, it would be highly desirable to numerically investigate the instability of the MBL phase, rather than its emergence from the thermal phase. In strongly disordered systems, the leading (proposed) instability of the localized phase is due to so called *avalanches* induced by rare thermal inclusions [17, 18]. The inclusions are extended regions where the disorder is anomalously small, as show in Fig. 1. Inclusions of any size ℓ_0 exist in the thermodynamic limit but, since they are exponentially unlikely in ℓ_0, one would need enormously large systems to observe and study them directly. Exact numerical studies are unfortunately limited to small system sizes and can therefore not directly capture these inclusions. One must thus find a way to induce avalanches in a controllable way, so they can be studied systematically. Instead of directly investigating rare thermal regions in a closed systems, we study the transient dynamics of a system coupled to an infinite bath, in line with a proposal by Moringstar et al. [19].

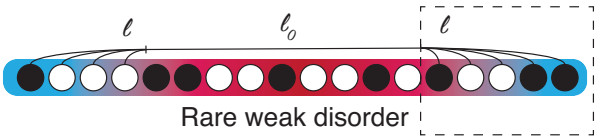

FIG. 1. **Rare thermal inclusion:** No matter how large the disorder, in the thermodynamic limit the system will contain regions of arbitrary size ℓ_0 where the disorder is so weak that it can effectively be neglected. In interacting systems, these rare regions serve as a heat bath for the rest of the system. The fate of the system depends critically on how fast particles in the vicinity of the bath thermalize with it. In this work we consider ideal asymptotically large baths $\ell_0 \to \infty$, such that all computational resources are used to describe the dynamics in the strongly disordered region ℓ of interest.

BATH INDUCED AVALANCHES

By connecting an infinite bath to a finite disordered chain, the system will surely thermalize. Within the avalanche picture [17, 18] it is the rate of thermalization that governs how large the thermal inclusions grow. Consider a spin chain with a thermal inclusion of size ℓ_0, as shown in Fig. 1, and imagine it has been able to thermalize ℓ spins on both sides, then the inclusion has grown to a size $\ell_0 + 2\ell$. Consequently, the level spacing of the inclusion has now become $\sim 2^{-(\ell_0+2\ell)}$. The inclusion can only serve as a proper bath as long as it thermalizes spins at a rate Γ which exceeds the level spacing, such that the spins can not resolve the discreteness of the spectrum of the bath before they thermalize. For a finite size system of length L, the critical thermalization rate to be stable against avalanches thus becomes $\Gamma \lesssim 4^{-L}$. The main purpose of this paper is to investigate the behavior of this thermalization rate Γ.

To study the relaxation rate, consider a system coupled to infinite Markovian bath such that the dynamics can be described by the following master equation

$$\partial_t \rho = \mathcal{L}(\rho), \tag{1}$$

with a Liouvillian super-operator

$$\mathcal{L}(\rho) = -i[H,\rho] + \gamma \sum_\mu \left(L_\mu \rho L_\mu^\dagger - \frac{1}{2}\left\{ L_\mu L_\mu^\dagger, \rho \right\} \right). \quad (2)$$

Here, H denotes the bare Hamiltonian of the system, L_μ specifies the nature of the coupling to the bath and γ simply denotes the nominal strength of the coupling. In what follows, I will consider the canonical disordered Heisenberg model

$$H = \frac{1}{4}\sum_{i=1}^{L-1} \vec{\sigma}_i \cdot \vec{\sigma}_{i+1} + \frac{1}{2}\sum_{i=1}^{L} h_i Z_i, \quad (3)$$

with h_i being i.i.d. random variables drawn out of uniform distribution on $[-W, W]$ and $\vec{\sigma}_i = (X_i, Y_i, Z_i)$ the vector composed of Pauli operator. To mimic the thermal inclusion, the Lindblad operators are taken to be the Pauli operators on the first spin, i.e. $L_\mu = (X_1, Y_1, Z_1)$. The solution to the Markovian master equation (1) is formally given by

$$\rho_t = \sum_i e^{\lambda_i t} p_i \rho_i, \quad (4)$$

where λ_i are the eigenvalues and ρ_i the right eigenoperators of the Liouvillian. The coefficients p_i denote the overlap of the initial state with the left eigenoperators of the Liouvillian. The stationary state, $\lambda_0 = 0$, will be unique and given by the infinite temperature ensemble $\rho_0 \propto \mathbb{I}$. The slowest decaying operator is associated with the eigenvalue with the second largest real part λ_1, its relaxation rate is given by $\Gamma = -\mathrm{Re}(\lambda_1)$.

Finding the exact spectrum of the Liouvillian superoperator is numerically quite demanding. It requires diagonalizing a $4^N \times 4^N$ matrix for a system composed of N spins and is thus limited to very small systems. In ref. [19] the coupling to the bath, γ in eq. (2), is taken to be of $O(1)$. However, at present, there is no immediate reason to be interested in non-perturbative effects of the system-bath coupling. In fact, at sufficiently large system-bath coupling one will induce a Zeno effect, resulting in a relaxation rate $\Gamma \propto 1/\gamma$. The virtue of working at weak coupling is that the decay rate can be computed perturbatively. For $\gamma = 0$, the eigenoperators and eigenvalues of the Liouvillian are simply given $\rho_{nm} = |n\rangle\langle m|$ and $\lambda_{nm} = i(E_m - E_n)$ respectively, where $|n\rangle$ and E_n denote the eigenvectors and eigenvalues of the bare Hamiltonian of the system. Assuming the Hamiltonian has no degenerate gaps, all the λ_{nm} are unique as long as $n \neq m$. There is an exponentially degenerate sector composed of all operators that are diagonal in the Hamiltonian, i.e. $n = m$ such that $\lambda_{nn} = 0$. It's easy to show that the slowest operator will be in this degenerate diagonal sector. For example, the perturbative decay rate of ρ_{nm} becomes $\Gamma_{nm} = \gamma \sum_\mu R_\mu$, with

$$R_\mu = \frac{1}{2}\left(\langle n|L_\mu^2|n\rangle + \langle m|L_\mu^2|m\rangle - 2\langle n|L_\mu|n\rangle\langle m|L_\mu|m\rangle \right).$$

It follows that $\Gamma_{nm} \geq (\Gamma_{mm} + \Gamma_{nn})/2$, implying one of the two diagonal states must have a smaller decay rate than the off-diagonal combination. The slowest operator thus resides in the diagonal sector and can be found by diagonalizing the matrix

$$M_{n,m} = \gamma \sum_\mu \left(\langle n|L_\mu^2|n\rangle \delta_{n,m} - |\langle n|L_\mu|m\rangle|^2 \right), \quad (5)$$

such that the decay rate is given by the smallest non-zero eigenvalue of M. Deep in the MBL phase, the latter can be thought of as the lifetime of the most decoupled l-bit. The computational cost has been reduced to diagonalizing a $2^N \times 2^N$ (dense) matrix. In fact, the relaxation rate of the slowest operator can also be found by minimizing:

$$\Gamma = \gamma \sum_\mu \frac{\mathrm{Tr}\left([O, L_\mu][L_\mu, O]\right)}{\mathrm{Tr}\left(O^2\right)}, \quad (6)$$

over all traceless operators that are constraint to be diagonal in the Hamiltonian H, i.e. $O = \sum_n o_n |n\rangle\langle n|$. In what follows, results for system sizes ranging from $L = 4$ to $L = 14$ will be discussed. Currently, numerics is limited by the precision with which one can represent the matrix elements of M. For this reason, we will use the 80th percentile instead of the median to characterize the typical behavior. Doing so does not affect the overall scaling behavior but allows us to study a slightly larger regime. To asses the stability against avalanches it's instructive to look at the crossing points of the ratio of the relaxation rate to the level spacing $g = \Gamma 4^L$ for various system sizes. The results are shown in Fig. 2 for the canonical disordered Heisenberg model. Over the range of available system sizes, the crossing point shifts from somewhere around $W \approx 7$ to $W > 20$, with no indication that this slows down in any way. This is in stark contrast to what happens in the non-interacting Anderson insulator where the crossing point barely moves (see Fig. 6 in Appendix A). On the same system sizes, a critical point of $W \approx 1.4$ is extracted, which is in good agreement with the avalanche stability threshold of $W = 1.34$ obtained by Crowley and Chandran [20].

Furthermore, the crossing in Fig. 2 becomes shallower with increasing system size, giving the impression that there is a lower bound to the rescaled rate g. This is exactly the behavior one would expect from a finite size crossover where small systems appear to become more stable to avalanches, i.e. g decreases with L, while ultimately crossing back over to a regime in which g increases with L, as shown in Fig. 3.

In other words, no exponentially localized conserved charges are found in the region that is accessible by state of the art numerics. If this behavior were to persist, there would be no stable MBL phase in the thermodynamic limit. To understand the drift it's instructive to analyze the asymptotic large W regime. Deep in the MBL phase

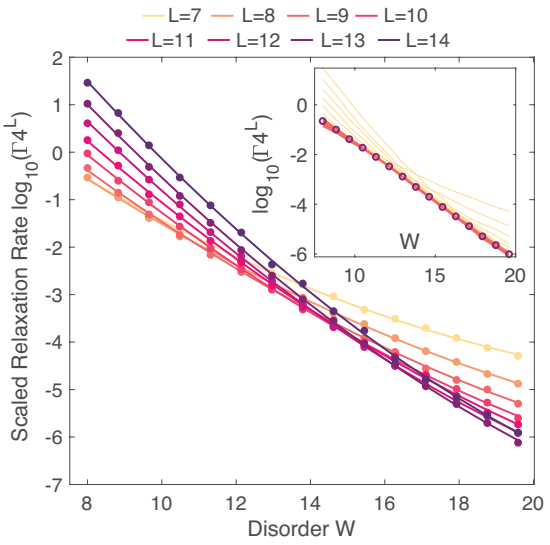

FIG. 2. **Relaxation rate:** Curves show the 80th percentile of the distribution of the smallest (non-zero) eigenvalue of the Liouvillian super-operator in a Heisenberg chain over disorder realizations. By rescaling with 4^L the crossing point in the data becomes indicative of the avalanche stability threshold. Different curves show different system sizes, ranging from $L = 7 - 14$. The crossing point drifts substantially from around $W^* \approx 8$ for the smallest system to $W^* > 20$ for the largest available system size. Inset shows the numerically extracted minimal value of $\Gamma 4^L$ with 99% bootstrap confidence intervals.

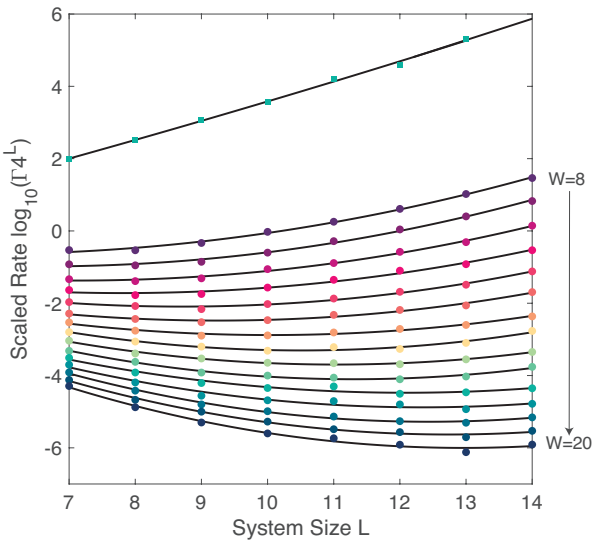

FIG. 3. **Relaxation rate II:** Curves show the behavior 80th percentile of the distribution of the smallest (non-zero) eigenvalue of the Liouvillian super-operator in a Heisenberg chain over disorder realizations. Different curves correspond to different value of the disorder strength $W = 8 - 20$; blue squares serve as a reference and correspond to weak disorder $W = 1$. Black lines show quadratic fits, from which we extract the minimal value of the rescaled rate shown in the inset in Fig. 2.

the thermalization rate of the system should be determined by the decay of the most distant l-bit from the bath. Reaching the bath than requires using $L-1$ bonds and if all those transitions are far of resonant one would expect the thermalization rate to scale as

$$\Gamma \approx \frac{C_L}{W^{2(L-1)}} \tag{7}$$

Such scaling can indeed be observed at much larger W, see Fig. 4. Due to limited numerical precision one can not access the asymptotic regime on larger system sizes. In order to extract the constant C_L, one can factor out the expected W^{2L-b} scaling and extrapolate the data to $W \to \infty$; numerically the constant b is found to be 2.8 which is close to the expected $b = 2$. The procedure is summarized in Fig. 4B. It's immediately clear that the constant C_L in expression (7) has a very strong dependence on the system size. The extracted constant, with bootstrapped confidence intervals, is shown in Fig. 5. It grows at least exponentially with system size, in contrast to the Anderson insulator in which it barely changes. In additional, there is a significant curvature on a semi-log scale, making the data much better described by a factorial rather than an exponential.

Thusfar the argument for the asymptotic $(J/W)^{2L-2}$-scaling, does not distinguish interacting from non-interacting problems, it simply captures the energetics of the problem but lacks the operator Hilbert space structure of the problem. For a non-interacting particle to reach the bath starting L sites away entails moving the particle one site in every step, implying there is a single path (Pauli string) contributing to the relaxation at leading order in $1/W$. Interacting particles can scatter with each other and this scattering process can lead to a rapid growth of the number of paths that contribute to the relaxation, i.e. the number of paths can grow much faster than exponential [10, 21–23]. It can of course not be ruled out from numerical considerations alone that at even higher disorder, the scaling of C_L becomes exponential in which case a stable MBL phase emerges. Regardless of the asymptotic behavior, the lower bound on the avalanche stability threshold is about four times larger than the current common consensus on the MBL transition.

Acknowledgments– I acknowledge useful discussions with A. Chandran, D. Huse and A. Polkovnikov. The Flatiron Institute is a division of the Simons Foundation. The work is partially supported by AFOSR: Grant FA9550-21-1-0236.

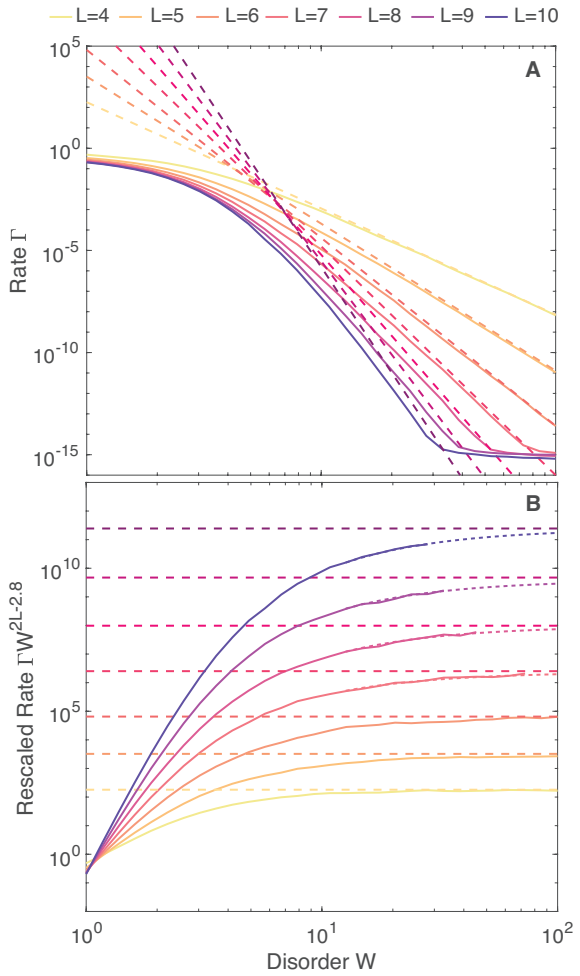

FIG. 4. **Relaxation rate III:** The typical slowest relaxing operator in a disordered Heisenberg chain. Curves show the 80th percentile of the distribution of the smallest (non-zero) eigenvalue of the Liouvillian super-operator over disorder realizations. Different curves correspond to different systems sizes ranging from $L = 4 - 10$. **Panel A** shows the bare rate Γ and **panel B** shows the rate rescaled by its expected asymptotic $W^{-2(L-1)}$ behavior. The dashed lines show the extracted asymptotes and dotted lines show the extrapolated function.

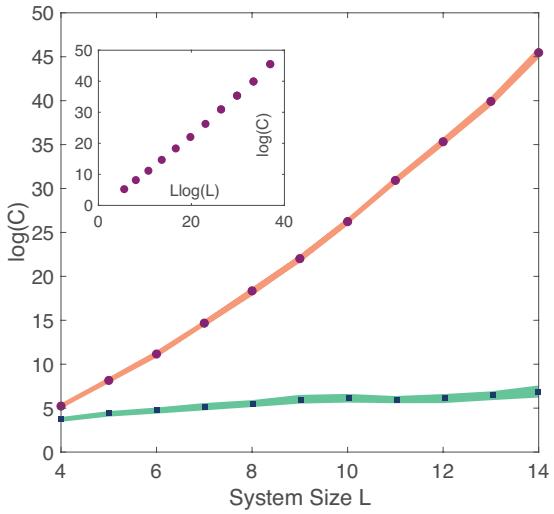

FIG. 5. **Asymptotic Scaling:** At sufficiently large disorder W the slowest relaxation rate is expected to behave as $C/W^{2(L-1)}$. This figure shows the change in the numerically extracted prefactor with system size L. Red circles and blue squares correspond to the Heisenberg chain and free fermions respectively. Shaded areas indicate 99% bootstrap confidence intervals. The inset shows the same data as a function of $L \log L$.

[1] R. Nandkishore and D. A. Huse, Many-body localization and thermalization in quantum statistical mechanics, Annu. Rev. Condens. Matter Phys. **6**, 15 (2015).
[2] D. A. Abanin, E. Altman, I. Bloch, and M. Serbyn, Colloquium: Many-body localization, thermalization, and entanglement, Rev. Mod. Phys. **91**, 021001 (2019).
[3] I. V. Gornyi, A. D. Mirlin, and D. G. Polyakov, Interacting electrons in disordered wires: Anderson localization and low-t transport, Phys. Rev. Lett. **95**, 206603 (2005).
[4] D. Basko, I. Aleiner, and B. Altshuler, Metal–insulator transition in a weakly interacting many-electron system with localized single-particle states, Annals of Physics **321**, 1126 (2006).
[5] V. Oganesyan and D. A. Huse, Localization of interacting fermions at high temperature, Phys. Rev. B **75**, 155111 (2007).
[6] J. Šuntajs, J. Bonča, T. Prosen, and L. Vidmar, Quantum chaos challenges many-body localization, Phys. Rev. E **102**, 062144 (2020).
[7] J. Šuntajs, J. Bonča, T. Prosen, and L. Vidmar, Ergodicity breaking transition in finite disordered spin chains, Phys. Rev. B **102**, 064207 (2020).
[8] M. Kiefer-Emmanouilidis, R. Unanyan, M. Fleischhauer, and J. Sirker, Slow delocalization of particles in many-body localized phases, Physical Review B **103**, 10.1103/physrevb.103.024203 (2021).
[9] D. Sels and A. Polkovnikov, Dynamical obstruction to localization in a disordered spin chain, Phys. Rev. E **104**, 054105 (2021).
[10] D. Sels and A. Polkovnikov, Thermalization of dilute impurities in one dimensional spin chains (2021), arXiv:2105.09348 [quant-ph].
[11] L. Vidmar, B. Krajewski, J. Bonča, and M. Mierzejewski, Phenomenology of spectral functions in disordered spin chains at infinite temperature, Phys. Rev. Lett. **127**, 230603 (2021).
[12] D. Abanin, J. Bardarson, G. De Tomasi, S. Gopalakrishnan, V. Khemani, S. Parameswaran, F. Pollmann, A. Potter, M. Serbyn, and R. Vasseur, Distinguishing localization from chaos: Challenges in finite-size systems, Annals of Physics **427**, 168415 (2021).
[13] P. Sierant, M. Lewenstein, and J. Zakrzewski, Polynomially filtered exact diagonalization approach to many-body localization, Physical Review Letters **125**, 10.1103/physrevlett.125.15660 (2020).
[14] D. J. Luitz and Y. B. Lev, Absence of slow particle transport in the many-body localized phase, Phys. Rev. B **102**, 100202 (2020).
[15] R. K. Panda, A. Scardicchio, M. Schulz, S. R. Taylor, and M. Žnidarič, Can we study the many-body localisation transition?, EPL (Europhysics Letters) **128**, 67003 (2020).
[16] P. J. D. Crowley and A. Chandran, A constructive theory of the numerically accessible many-body localized to thermal crossover (2021), arXiv:2012.14393 [cond-mat.dis-nn].
[17] W. De Roeck and F. m. c. Huveneers, Stability and instability towards delocalization in many-body localization systems, Phys. Rev. B **95**, 155129 (2017).
[18] T. Thiery, M. Müller, and W. D. Roeck, A microscopically motivated renormalization scheme for the mbl/eth transition (2017), arXiv:1711.09880 [cond-mat.stat-mech].
[19] A. Morningstar, L. Colmenarez, V. Khemani, D. J. Luitz, and D. A. Huse, Avalanches and many-body resonances in many-body localized systems, Phys. Rev. B **105**, 174205 (2022).
[20] P. J. D. Crowley and A. Chandran, Avalanche induced coexisting localized and thermal regions in disordered chains, Phys. Rev. Research **2**, 033262 (2020).
[21] A. Avdoshkin and A. Dymarsky, Euclidean operator growth and quantum chaos, Phys. Rev. Research **2**, 043234 (2020).
[22] X. Cao, A statistical mechanism for operator growth, Journal of Physics A: Mathematical and Theoretical **54**, 144001 (2021).
[23] D. E. Parker, X. Cao, A. Avdoshkin, T. Scaffidi, and E. Altman, A Universal Operator Growth Hypothesis, Phys. Rev. X **9**, 041017 (2019).

APPENDIX A: ANDERSON INSULATOR

To further substantiate the method, it's instructive to investigate the Anderson insulator over the same range of system sizes and disorder strengths as the results presented on the Heisenberg model in the main text. It serves as a point of comparison. Specifically, consider the Hamiltonian

$$H = \frac{1}{4}\sum_{i=1}^{L-1}(X_iX_{i+1} + Y_iY_{i+1}) + \frac{1}{2}\sum_{i=1}^{L} h_iZ_i, \tag{8}$$

with h_i being i.i.d. random variables drawn out of uniform distribution on $[-W, W]$ and (X_i, Y_i, Z_i) denoting the respective Pauli operators on each site i. After Jordan-Wigner transformation this maps to free fermions with on-site disorder. A detailed analysis by Crowley and Chandran [20] concluded that the Anderson insulator should be stable against avalanches for disorder strengths $W > 1.34$. Even on very small systems I find $W^* \approx 1.4$, with a crossing that

drifts very weakly to smaller values of disorder, see Fig. 6. Note that at fixed disorder one observes a rather clean exponential growth/decay for the rescaled rate $\Gamma 4^L$, in contrast to the observed crossover behavior in the Heisenberg model.

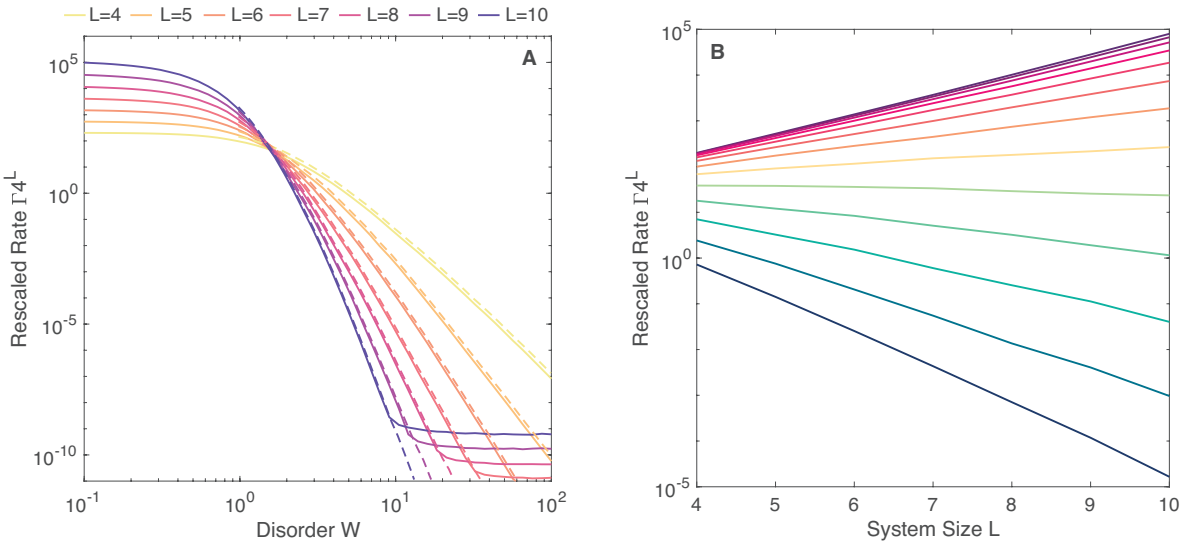

FIG. 6. **Relaxation time Anderson:** The typical slowest relaxing operator in a disordered chain of non-interacting fermions. Curves show the 80th percentile of the distribution of the smallest (non-zero) eigenvalue of the Liouvillian super-operator over disorder realizations. **Panel A** Different curves correspond to different systems sizes ranging from $L = 4 - 10$. By rescaling with 4^L the crossing point in the data becomes indicative of the avalanche stability threshold. A stable crossing is observed around $W \approx 1.4$. The dashed lines show the decay rate of the slowest single particle operator. **Panel B** The same data is shown as a function of L for different values of the disorder strength W.